Neutron field characteristics of Ciemat's Neutron Standards Laboratory

Karen A. Guzman-Garcia [a,*], Roberto Mendez-Villafañe [b], Hector Rene Vega-Carrillo [c]

[a] Universidad Politécnica de Madrid. C. José Gutierrez Abascal, 2, 28006 Madrid, Spain
[b] Centro de Investigaciones Energeticas, Medioambientales y Tecnologicas, CIEMAT, Avenida Complutense, 40, 28040 Madrid, Spain
[c] Unidad Académica de Estudios Nucleares de la UAZ, C. Cipres, 10, 98068 Zacatecas, Mexico

HIGHLIGHTS

- ^{241}AmBe and ^{252}Cf are the standards at the LPN-CIEMAT.
- Monte Carlo method was used to characterize the sources.
- A detailed model of source, bench and room was designed.
- Neutron spectra, fluences and $H^*(10)$ were estimated on the bench.

ABSTRACT

Monte Carlo calculations were carried out to characterize the neutron field produced by the calibration neutron sources of the Neutron Standards Laboratory at the Research Center for Energy, Environment, and Technology (CIEMAT) in Spain. For ^{241}AmBe and ^{252}Cf neutron sources, the neutron spectra, the ambient dose equivalent rates and the total neutron fluence rates were estimated. In the calibration hall, there are several items that modify the neutron field. To evaluate their effects different cases were used, from point-like source in vacuum up to the full model. Additionally, using the full model, the neutron spectra were estimated to different distances along the bench; with these spectra, the total neutron fluence and the ambient dose equivalent rates were calculated. The hall walls induce the largest changes in the neutron spectra and the respective integral quantities. The free-field neutron spectrum is modified due the room return effect.

Keywords:
Neutron
Monte Carlo
Spectra
Standard

1. Introduction

Neutrons in the ambient environment are produced during cosmic ray interactions with the nuclei in the atmosphere (Miloshevsky and Hassanein, 2014, Pioch et al., 2011) and in the Earth's crust (Vega-Carrillo and Manzanares, 2004). Neutrons are also produced in nuclear reactors, particle accelerators or by mixing an α or γ-rays emitter radioisotope with a suitable material inducing (α, n) or (γ, n) nuclear reactions (Vega-Carrillo et al., 2009).

In various areas, including medicine, power generation, the nuclear fuel cycle, national security, radiation protection, etc., neutrons are intentionally or inherently produced for research, as a technological tool, or for teaching purposes. In all these cases, it is important to measure the neutrons as well as their dosimetric magnitudes. However, such measurements have drawbacks because neutrons can be found in a wide energy range with different intensities and angular distributions, are commonly accompanied with gamma rays, have an energy-dependent interaction with matter and because there are limitations in the response of neutron measuring devices (Lacoste, 2010, Schuhmacher, 2004).

Calibration of dosimeters and neutron monitoring instruments is carried out using reference neutron fields with broad spectral distributions (Gressier, 2014, Nolte et al., 2004), under controlled conditions (Pereira et al., 2014). In Spain, responsibility for this falls on the Metrology Laboratory of Ionizing Radiation of the Research Center for Energy, Environment, and Technology (LMRI-CIEMAT). Due to this, a new facility called the Neutron Standards Laboratory, LPN, of CIEMAT was designed and built (Méndez-Villafañe et al., 2014). The main purpose of the LPN is to be a primary reference laboratory of neutron measurements in Spain, with the aim of give service to the neutron users in the nuclear industry, health and research institutions where neutrons are produced.

* Corresponding author.
E-mail addresses: ingkarenguzman@gmail.com (K.A. Guzman-Garcia), roberto.mendez@ciemat.es (R. Mendez-Villafañe), fermineutron@yahoo.com (H.R. Vega-Carrillo).

A neutron calibration facility has neutron sources that provide neutron fields whose spectra and doses, are well known at the calibration points (Gressier, 2014). In these facilities, neutrons are scattered by air, floor, walls, support structures and the source cladding, contributing significantly to the neutron field influencing the readout of the instrument to be calibrated (Pereira et al., 2014). To ensure reliable results in dosimetry, calibration, and irradiation with neutrons, it is necessary to characterize the neutron field in the facility (Gallego et al., 2004; Tripathy et al., 2009).

The aim of this study was to characterize the neutron field in the LPN-CIEMAT using Monte Carlo methods. In the characterization the neutron spectra and the ambient dose equivalent were estimated using different models for the neutron sources and the calibration hall.

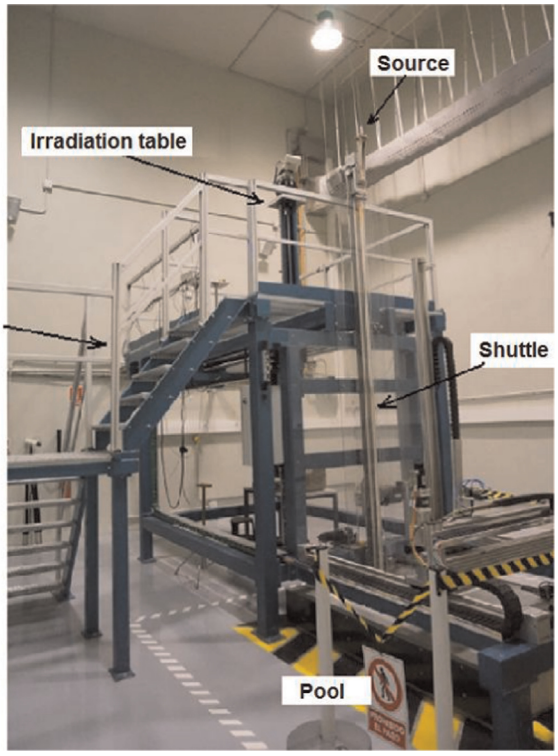

Fig. 2. Bench, pool, irradiation table, source and shuttle.

2. Materials and methods

2.1. Neutron Standards Laboratory

The LPN has a hall (9 m × 7.5 m × 8 m) with 150 cm-thick concrete walls. In the floor, there is a water-filled pool (150 cm × 100 cm × 150 cm) with walls coated with high density polyethylene. On the top, the pool has a door made of concrete; the pool is used to store the neutron sources. The calibration hall has a stainless steel bench that is 250 cm high by 375 cm long, having an irradiation bedplate where the device to be calibrated is fixed with respect to the center of the source. Fig. 1 (Méndez-Villafañe et al., 2014) shows a side view of the calibration hall with the bedplate (irradiation table) and the water pool.

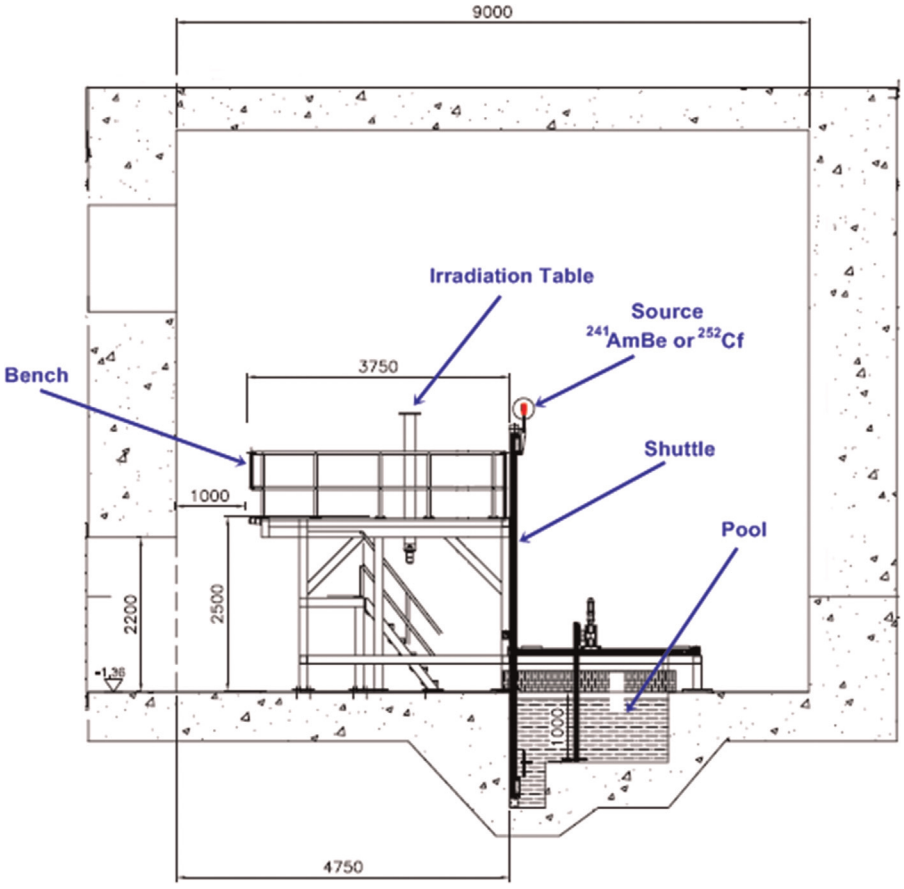

Fig. 1. Side view of LPN-CIEMAT, dimensions are in mm.

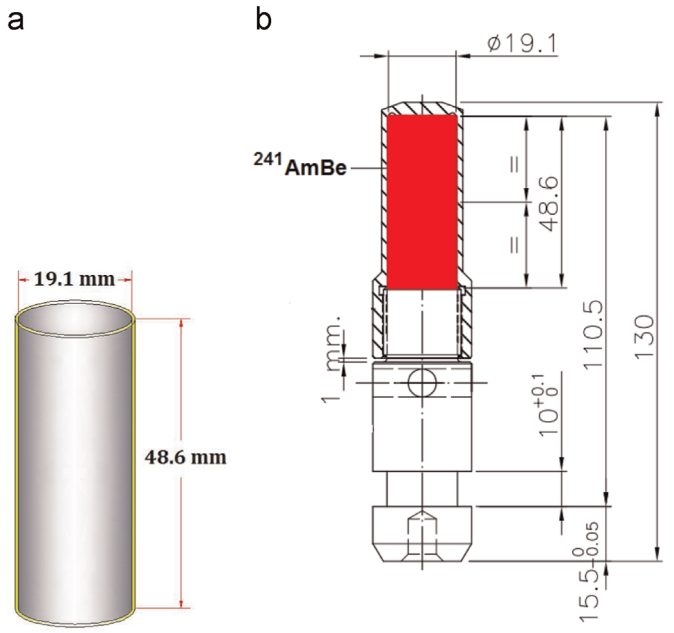

Fig. 3. ^{241}AmBe source double capsule (a) and capsule holder (b), dimensions are in mm.

The bench was designed to align the center of any neutron measuring device with the center of the neutron source in any position from 50 up to 370 cm. To reduce the neutron scattering in the irradiation position, the center of the source is located approximately in the center of the calibration hall, being 4 m above the floor (Pereira et al., 2014). A shuttle device is used to move the sources from the pool to the calibration bench.

Fig. 2 (CIEMAT, 2013) shows the LPN image, with the bench, the source, the irradiation table (bedplate), the shuttle and the pool.

The LPN has two neutron calibration sources, ^{241}AmBe and ^{252}Cf, recommended by the International Organization for Standarization (ISO, 2008), for monitor and dosimeter calibration purposes. The mean energy of neutrons emitted by the ^{241}AmBe

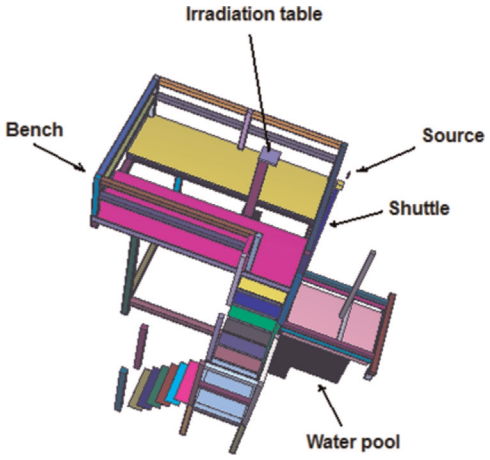

Fig. 5. Bench and pool model.

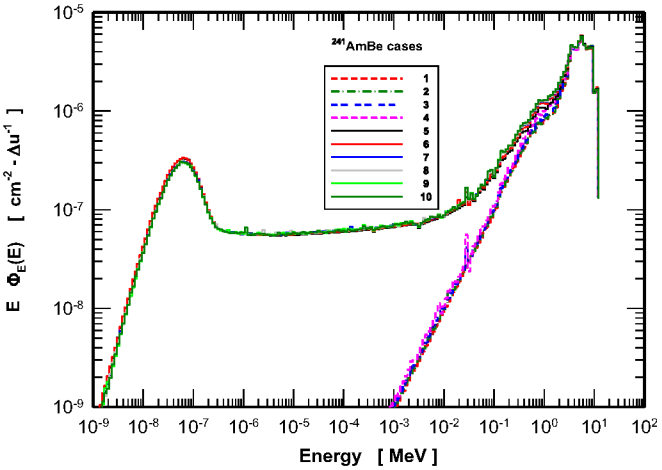

Fig. 6. Neutron lethargy spectra, at 100 cm from ^{241}AmBe, for all the cases.

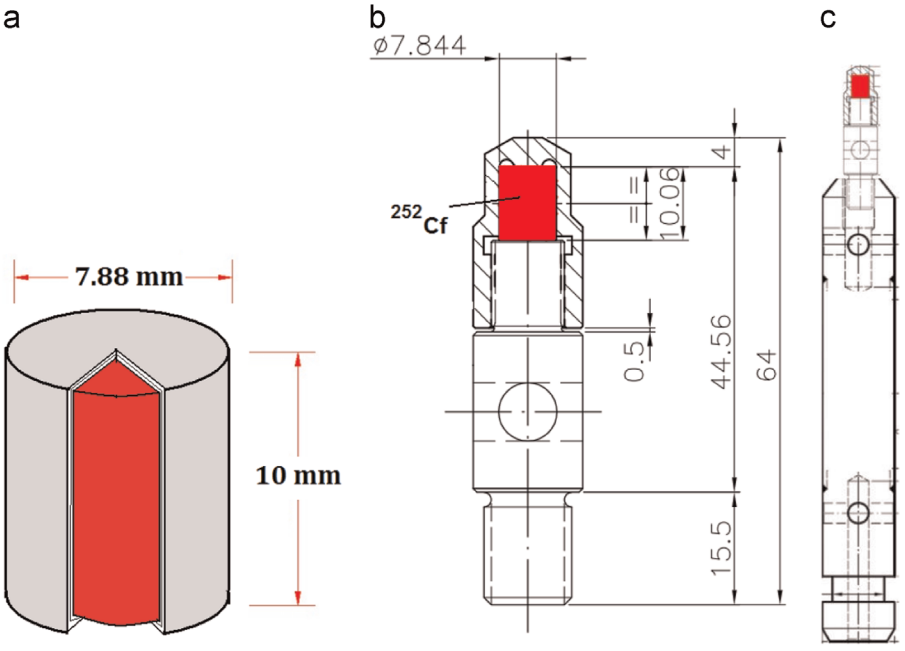

Fig. 4. ^{252}Cf source (a), the capsule holder (b), and the capsule cart holder (c), dimensions are in mm.

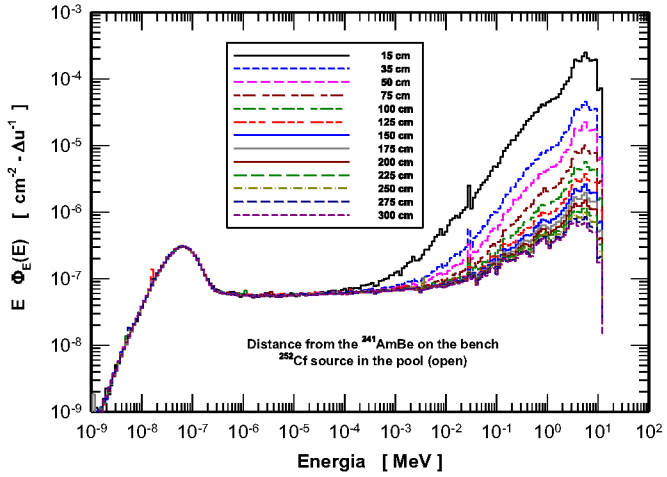

Fig. 7. Neutron lethargy spectra at different distance from the ^{241}AmBe source with the ^{252}Cf in the pool (open).

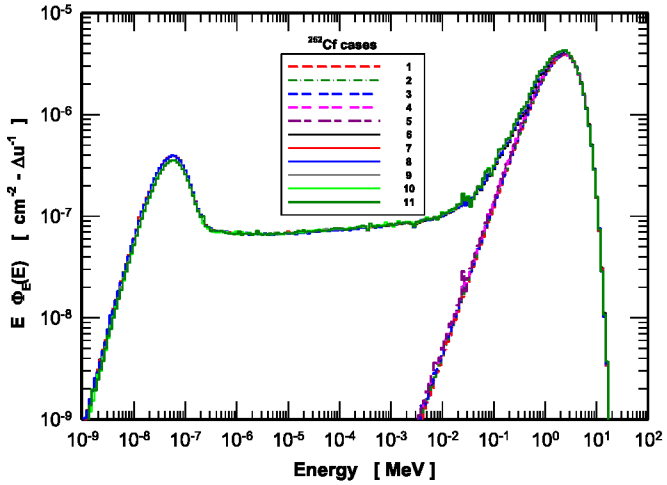

Fig. 8. Neutron lethargy spectra, at 100 cm from ^{252}Cf, for all the cases.

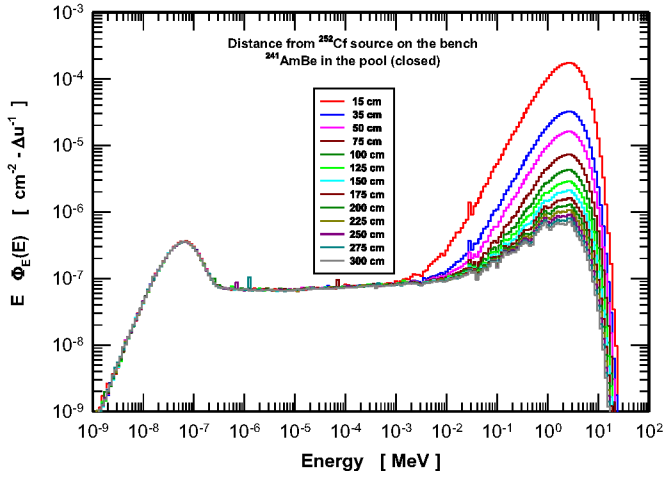

Fig. 9. Neutron lethargy spectra at different distance from the ^{252}Cf source with the ^{241}AmBe in the pool (closed).

source is 5 MeV; this source has a long half-life. The average energy of ^{252}Cf neutrons is 2.13 MeV, and it has a large specific activity; however, it has a half-life of 2.65 y and should be replaced on a regular basis (Schuhmacher, 2004, Vega-Carrillo et al., 2009).

Table 1

$\dot{H}^*(10)$ at 100 cm from the ^{241}AmBe source, for all the cases.

Case	$\dot{H}^*(10)$ [μSv/h]
1	124
2	124
3	126
4	128
5	137
6	140
7	142
8	142
9	144
10	144

Table 2

$\dot{H}^*(10)$ at 100 cm from the ^{252}Cf source, for all the cases.

Case	$\dot{H}^*(10)$ [μSv/h]
1	6402
2	6458
3	6473
4	6587
5	6613
6	7103
7	7213
8	7237
9	7359
10	7467
11	7465

The ^{241}AmBe source has a nominal activity of 185 GBq and emits $1.110 \times 10^7 \pm 1.4\%$ s^{-1}, traceable to the Czech Metrology Institute. The sources is americium oxide, mainly ^{241}Am, dispersed in a matrix of beryllium metal powder encapsulated in 2 mm-thick welded A316 stainless steel. This source is a cylinder, 19.1 mm in diameter and 48.6 mm high, as shown in Fig. 3.

The californium source has 250 μg of ^{252}Cf; the nominal activity is 5 GBq and emits $5.471 \times 10^8 \pm 2.6\%$ s^{-1}, traceable to the National Institute of Standards and Technology. This source is a cylinder that is 7.8 mm in diameter and 10.0 mm high. The californium is dispersed in a ceramic matrix encapsulated in 2 mm-thick A316 stainless steel to ensure its integrity under all conditions. The source is enclosed within a capsule that is manipulated with a needle cartridge. The details of this source are shown in Fig. 4.

2.2. Monte Carlo calculations

Calculations were carried out with the MCNPX code, version 2.6.0 (Pelowitz, 2005), where a detailed model of the LPN was used. In the model, those elements that impact the neutron transport were included, such as the source's features, the bench, the irradiation bedplate, the source's support, and the water pool. Fig. 5 shows the bench and the pool model.

To evaluate the effect on the neutron features due to the different elements in the LPN, calculations were made for both sources using different cases. The cases for the ^{241}AmBe source were as follows:

Case 1: Point-like source in vacuum.
Case 2: Point-like source in air.
Case 3: Real source in air and the double ^{241}AmBe capsule.
Case 4: Real source in the source's holder.
Case 5: Real source, without the source's holder, and the room.

Table 3
Neutron fluence rates, at different distances from the ^{241}AmBe source, for all the cases.

Distance [cm]	ϕ_1 [cm^{-2} s^{-1}]	ϕ_2 [cm^{-2} s^{-1}]	ϕ_3 [cm^{-2} s^{-1}]	ϕ_4 [cm^{-2} s^{-1}]	ϕ_5 [cm^{-2} s^{-1}]	ϕ_6 [cm^{-2} s^{-1}]	ϕ_7 [cm^{-2} s^{-1}]	ϕ_8 [cm^{-2} s^{-1}]	ϕ_9 [cm^{-2} s^{-1}]	ϕ_{10} [cm^{-2} s^{-1}]
15	3891	3896	3937	4032	3963	4057	4060	4063	4063	4063
35	715	717	725	743	750	768	770	772	772	772
50	350	352	356	365	381	390	392	394	394	394
75	156	155	158	162	184	188	190	191	191	191
100	88	87	89	91	114	117	118	119	120	120
125	56	57	57	59	82	84	85	85	87	87
150	39	39	40	41	65	66	67	67	69	69
175	29	29	29	30	54	55	56	56	57	57
200	22	22	22	23	47	48	49	49	49	49
225	17	18	18	18	43	43	44	44	44	44
250	14	14	14	15	39	40	41	40	41	41
275	12	12	12	12	37	37	38	38	38	38
300	10	10	10	10	35	36	36	36	36	36

Table 4
Neutron fluence rates, at different distances from the ^{252}Cf source, for cases 3–10.

Distance [cm]	ϕ_3 [cm^{-2} s^{-1}]	ϕ_4 [cm^{-2} s^{-1}]	ϕ_5 [cm^{-2} s^{-1}]	ϕ_6 [cm^{-2} s^{-1}]	ϕ_7 [cm^{-2} s^{-1}]	ϕ_8 [cm^{-2} s^{-1}]	ϕ_9 [cm^{-2} s^{-1}]	ϕ_{10} [cm^{-2} s^{-1}]
15	208474	209247	205951	210034	210813	210912	211126	211128
35	38390	38552	39186	39953	40096	40201	40336	40336
50	18842	18923	20023	20403	20473	20571	20668	20666
75	8392	8428	9780	9953	10046	10067	10143	10139
100	4730	4751	6189	6287	6301	6377	6462	6457
125	3032	3045	4523	4587	4597	4670	4776	4768
150	2108	2116	3615	3661	3662	3726	3811	3804
175	1549	1556	3065	3099	3098	3153	3197	3195
200	1187	1192	2707	2734	2733	2778	2801	2796
225	938	942	2461	2484	2489	2527	2531	2530
250	759	762	2284	2305	2308	2336	2336	2335
275	627	630	2156	2173	2177	2199	2194	2191
300	526	528	2059	2075	2077	2093	2081	2079

Case 6: Real source in the source's holder, and the room.
Case 7: Real source in the holder, 4 m above floor with the bench.
Case 8: Real source in the holder, 4 m above floor with the bench and the shuttle.
Case 9: Same as case 7 but including the irradiation table and the ^{252}Cf source in the pool (closed).
Case 10: Same as case 9, but the pool was open.

The calculated cases for the ^{252}Cf source were as follows:

Case 1: Point-like source in vacuum.
Case 2: Point-like source in air.
Case 3: Real source in air with ^{252}Cf within double capsule.
Case 4: Same as case 3 but in the source's holder.
Case 5: Same as case 4 but including the capsule holder cart.
Case 6: Same as case 3 but with the source 4 m above floor and the room.
Case 7: Same as case 5 but with the source 4 m above floor and the room.
Case 8: Same as case 7 but including the holder capsule cart.
Case 9: Same as case 8 but with the bench.
Case 10: Same as case 9 but with the irradiation table, source's shuttle, and the ^{241}AmBe in the pool (closed).
Case 11: Same as case 10 but with the pool open.

For these cases, a point detector was located at 100 cm from the source, and the neutron spectra, $\Phi_E(E)$, were estimated to evaluate the effect of the different components of the calibration facility. The $\Phi_E(E)$ was used to calculate the ambient dose equivalent rate, $\dot{H}^*(10)$, using Eq. (1) (Gallego et al., 2004).

$$\dot{H}^*(10) = Q \int_E \Phi_E(E)\, h^*(10)\, dE \tag{1}$$

In this equation, Q is the source strength and $h^*(10)$ are the fluence-to-ambient dose equivalent conversion coefficients obtained from the report 74 of the International Commission on Radiological Protection (ICRP, 1996).

Using the complete model, case 10, the MCNPX code was also used to estimate the neutron spectra, $\Phi_E(E)$, on the irradiation table at 15, 35, 50, 75, 100, 125, 150, 175, 200, 225, 250, 275 and 300 cm from the source. For the ^{241}AmBe source, the spectra were estimated with the ^{252}Cf in the water pool with the pool open. For the ^{252}Cf source, the spectra were estimated with the ^{241}AmBe in the pool, which was closed. The $\Phi_E(E)$ were used to calculate the total neutron fluence rate, ϕ, using Eq. (2) (Gallego et al., 2004).

$$\phi = Q \int_E \Phi_E(E)\, dE \tag{2}$$

For all cases, the number of Monte Carlo histories was large enough to reach an uncertainty less than 3%.

3. Results

Fig. 6 shows the calculated neutron spectra at 100 cm from the ^{241}AmBe source for all the cases.

The ^{241}AmBe neutron spectra calculated at different distances, with the ^{252}Cf source in the pool (open), are shown in Fig. 7.

Fig. 8 shows the calculated neutron spectra at 100 cm from the ^{252}Cf source for all the cases.

The ^{252}Cf neutron spectra calculated at different distances with the ^{241}AmBe source in the pool (closed) are shown in Fig. 9.

In Table 1, the $\dot{H}^*(10)$ at 100 cm from the ^{241}AmBe for all the cases are shown, in Table 2, the $\dot{H}^*(10)$ at 100 cm from the ^{252}Cf source are shown.

Tables 3 and 4 show the total neutron fluence rates at different distances from the ^{241}AmBe and ^{252}Cf sources, respectively. For ^{241}AmBe, all cases are shown; for ^{252}Cf, case 3 to case 10 are shown.

4. Discussion

Neutron spectra change significantly when the floor, ceiling and walls of the room are included in the model (Figs. 6 and 8); in the spectra the epithermal and thermal neutrons are due the room-return effect (Vega-Carrillo et al., 2007a). The changes in the spectra due to the presence of the bench and the pool are not significant.

As the distance from the neutron source increases, the number of neutrons with energy larger than 10^{-3} MeV decreases; on the other hand, the number of neutrons with energy less than 10^{-3} MeV remains constant (Figs. 7 and 9). To 15 cm from the ^{241}AmBe source, this effect is different; here, the neutron energy borderline is shifted to 10^{-4} MeV; the probable explanation is due to the differences in the neutron mean energies of the sources. The average neutron energy of the ^{241}AmBe source is 5 MeV whereas it is 2.13 MeV for ^{252}Cf; thus, at short distances (< 15 cm) from ^{241}AmBe, a neutron require a larger number of interactions to be moderated and eventually thermalized due to room-return (Vega-Carrillo et al., 2007b).

Table 1 shows the $\dot{H}^*(10)$ at 100 cm from the ^{241}AmBe source. Comparing the $\dot{H}^*(10)$ at 100 cm from the ^{241}AmBe source using the complete model (case 10) with the dose with the real source in a free-field (case 3), there is an increase of 14.3% due to the neutron scattering.

For cases 1 and 2, the $\dot{H}^*(10)$ are the same; therefore, at 100 cm the neutron skyshine in air is absent. When the real source is used (case 3), the dose increases 1.6% in comparison with the point-like case due to the source´s size and neutron scattering in the capsule.

Comparing cases 4 and 3, the $\dot{H}^*(10)$ increases 1.6% due the neutron scattering in the source's holder. When the room (floor, ceiling, and walls) is included in the model (cases 4 and 6), the dose increases 9.4%; this effect is similar to the effect reported in literature (Gallego et al., 2004, Pereira et al., 2014).

The $\dot{H}^*(10)$ increases 1.4% when the bench is included in the room (cases 6 and 7); the inclusion of the source shuttle has no influence (cases 7 and 8). When the pool is included (case 9), the dose increases 1.4% in comparison with case 8.

Comparing the $\dot{H}^*(10)$ for cases 9 and 10, there is no difference, meaning that the amount of neutrons leaking out from the pool does not affect the dose at 100 cm from the source on the bench.

Table 2 shows the values of $\dot{H}^*(10)$ at 100 cm from the ^{252}Cf source. Comparing the $\dot{H}^*(10)$ at 100 cm from the ^{252}Cf source using the complete model (case 10) with the dose with the real source in a free-field (case 3), there is an increase of 15.4% due to the neutron scattering.

For cases 1 and 2, the $\dot{H}^*(10)$ with the source in air is 0.9% larger than the source in vacuum. This difference is less than the Monte Carlo calculations uncertainties; therefore, this difference is meaningless. The same occurs when the real source is used (case 3) most likely due to the source size. However, when the source's holder is included, the dose increases 1.8% (comparing case 3 and 4) but the inclusion of the cart (case 5) has no effect in the $\dot{H}^*(10)$.

Comparing cases 5 and 6, the $\dot{H}^*(10)$ increases 7.4% due to the inclusion of the floor, ceiling and walls of the hall; these items induce the largest changes in the spectra.

Comparing cases 6 and 7, the $\dot{H}^*(10)$ increases 1.5% due to the inclusion of the source's holder in the model with the room. The bench has no effect on the dose (cases 7 and 8). When the pool is included (case 11), the dose increases 1.4% in comparison with case 9. Comparing the $\dot{H}^*(10)$ for cases 9 and 10, the difference is meaningless; thus, the amount of neutrons leaking out from the pool does not affect the dose at 100 cm from the source on the bench, as was noticed with the ^{241}AmBe source.

The neutron fluence rates for all cases at different distances from the ^{241}AmBe (Table 3) decrease as the distance increases. Comparing cases 4 and 5, the inclusion of the room (case 5) at 50 cm from the source increases the ϕ by 4.4%; at 100 cm, the increase is 25.3%. For larger distances, the room (case 5) induces larger increases in the ϕ in comparison to when the room is not included (case 4); thus, the ϕ is 2.04 and 3.50 times larger at 200 and 300 cm, respectively. Similar effects have been reported by .

Comparing the ϕ with the full model (case 10) with the real source in a free field (case 3) at 100 cm, in can be notice an increases of 34.8%. At 200 and 300 cm, the ϕ for case 10 is 2.22 and 3.60 times larger, respectively, when is compared with the case 3.

For the ^{252}Cf source (Table 4), the inclusion of the room with the source (case 6) at 50 cm from the source compared to without the room (case 4) increases the ϕ by 7.8%; at 100 cm the increase is 32.3%. For the larger distances of 200 and 300 cm, the ϕ is 2.29 and 3.93 times larger, respectively, when the room is included (case 6) in comparison with the case without the room (case 4). Similar trends, with a ^{252}Cf source in a low scattering metrology laboratory, have been reported (Pereira et al., 2014).

The use of the full model (case 10) in comparison with the real source (case 3) in a free field at 50 cm increases the ϕ by 9.7%, at 100 cm, the increase is 36.5%.

5. Conclusions

To characterize the neutron field produced by the calibration sources of the LPN-CIEMAT, the neutron spectra were estimated in various points on the bench using different cases. With the neutron spectra and the source strengths, the $\dot{H}^*(10)$ and the total neutron fluences were also estimated.

The walls of the LPN induce the largest changes in the neutron spectra due to the room return effect. Regardless of the neutron source, as the distance from the source increases, the amount of neutrons with $E > 10^{-3}$ MeV is reduced. On the other hand, those neutrons with energy less than 10^{-3} MeV remain constant.

When one source is in the irradiation position on the bench and another source is in the pool, the spectra, the neutron fluence rates and the ambient doses equivalent rate are not affected regardless of whether the pool´s door is open or closed.

Acknowledgments

KA Guzman-Garcia thanks the scholarship granted by the Spanish Agency for International Cooperation for the Development.

References

CIEMAT, 2013. El Laboratorio de Patrones Neutrónicos comienza a funcionar como referencia nacional. Centro de Investigaciones Energéticas, Medioambientales y Tecnológicas. ⟨http://www.ciemat.es/portal.do?IDM=61&NM=2&identificador=301⟩ [online, reviewed on February 2014].

Gallego, E., Lorente, A., Vega-Carrillo, H.R., 2004. Characteristics of the neutron fields on the facility at DIN-UPM. Radiat. Prot. Dosim. 110, 73–79.

Gressier, V., 2014. Review of neutron calibration facilities and monitoring techniques: new needs for emerging fields. Radiat. Prot. Dosim. 161, 27–36.

ICRP, 1996. Conversion coefficients for use in radiological protection against external radiation. ICRP Publication 74. Ann. ICRP 26, 199.

ISO, 2008. Reference Radiation Fields – Simulated workplace neutron fields – Part 2: Calibration fundamentals related to the basic quantities. International Organization for Standardization, Geneva (ISO Standard 12789-2).

Lacoste, V., 2010. Review of radiation sources, calibration facilities and simulated workplace fields. Radiat. Meas. 45, 1083–1089.

Méndez-Villafañe, R., Guerrero, J.E., Embid, M., Fernández, R., Grandio, R., Pérez-Cejuela, P., Márquez, J.L., Alvarez, F., Ortego, P., 2014. Design and verification of the shielding around the new neutron standards laboratory (LPN) at CIEMAT. Radiat. Prot. Dosim. 161, 393–397.

Miloshevsky, G., Hassanein, A., 2014. Time correlation of cosmic ray-induced neutrons and gamma rays at sea level. Nucl. Instrum. Methods Phys. Res. A 737, 33–41.

Nolte, R., Allie, M.S., Böttger, R., Brooks, F.D., Buffler, A., Dangendorf, V., Friedrich, H., Guldbakke, S., Kein, H., Meulders, J.P., Schlegel, D., Schuhmacher, H., Smit, F.D., 2004. Quasi-monoenergetic neutron reference fields in the energy range from thermal to 200 MeV. Radiat. Prot. Dosim. 110, 97–102.

Pelowitz, D.B., 2005. MCNPX User's Manual. Los Alamos National Laboratory Report LA-CP-05-0369. Los Alamos, NM.

Pereira, M., Salgado, A.P., Filho, A.S., Pereira, W.W., Patrao, K.C.S., Fonseca, E.S., 2014. Neutron metrology laboratory facility simulation. Radiat. Protect. Dosim. , http://dx.doi.org/10.1093/rpd/ncu164.

Pioch, C., Mares, V., Vashenyuk, E.V., Balabin, Y.V., Ruhm, W., 2011. Measurement of cosmic ray neutrons with Bonner sphere spectrometer and neutron monitor at 79°N. Nucl. Instrum. Methods Phys. Res. A 626–627, 51–57.

Schuhmacher, H., 2004. Neutron calibration facilities. Radiat. Prot. Dosim. 110, 33–42.

Tripathy, S.P., Bakshi, A.K., Sathian, V., Tripathi, S.M., Vega-Carrillo, H.R., Nandy, M., Sarkar, P.K., Sharma, D.N., 2009. Measurements of ^{241}AmBe spectra (bare and Pb-covered) using TLD pairs in multi-spheres: spectrum unfolding by different methods. Nucl. Instrum. Methods Phys. Res. A 598, 556–560.

Vega-Carrillo, H.R., Manzanares, E., 2004. Background neutron spectrum at 2420 m above sea level. Nucl. Instrum. Methods Phys. Res. A 524, 146–151.

Vega-Carrillo, H.R., Manzanares, E., Iñiguez, M.P., Gallego, E., Lorente, A., 2007a. Study of room-return neutrons. Radiat. Meas. 42, 413–419.

Vega-Carrillo, H.R., Manzanares, E., Iñiguez, M.P., Gallego, E., Lorente, A., 2007b. Spectrum of isotopic neutron sources inside concrete walls spherical cavities. Radiat. Meas. 42, 1373–1379.

Vega-Carrillo, H.R., Martinez-Blanco, M.R., Hernandez-Davila, V.M., Ortiz-Rodriguez, J.M., 2009. Spectra and dose with ANN of ^{252}Cf, ^{241}AmBe, and ^{239}PuBe. J. Radioanal. Nucl. Chem. 281, 615–618.